Available online at www.sciencedirect.com

SciVerse ScienceDirect

Ceramics International 39 (2013) 5901–5907

CERAMICS INTERNATIONAL

www.elsevier.com/locate/ceramint

Liquefied petroleum gas sensing performance of cerium doped copper ferrite

M.S. Khandekar[a], N.L. Tarwal[b,c], J.Y. Patil[a], F.I. Shaikh[a], I.S. Mulla[d], S.S. Suryavanshi[a,*]

[a]Ferrite Materials Laboratory, Department of Physics, Solapur University, Solapur, India
[b]Research Institute for Solar and Sustainable Energies (RISE), Gwangju Institute of Science and Technology (GIST), Gwangju 500712, Republic of Korea
[c]School of Information and Communications, Gwangju Institute of Science and Technology (GIST), Gwangju 500712, Republic of Korea
[d]Physical Chemistry Division, National Chemical Laboratory, Pune 411008, India

Received 12 October 2012; received in revised form 24 December 2012; accepted 6 January 2013
Available online 20 January 2013

Abstract

Undoped and cerium (Ce) doped nanocrystalline copper ferrite ($CuFe_2O_4$) materials were synthesized via the molten-salt (M-S) method. Effects of Ce doping on the structural, morphological and gas sensing properties of the $CuFe_2O_4$ ferrite have been investigated. X-ray diffraction (XRD) analysis revealed the formation of spinel $CuFe_2O_4$. Scanning electron microscopy (SEM) and transmission electron microscopy (TEM) investigations showed that the synthesized ferrite is made up of very fine spherical nanoparticles. Moreover, the gas sensing properties of sintered samples were studied towards different reducing gases such as liquefied petroleum gas (LPG), acetone, ethanol and ammonia. The sample with 4% cerium doped $CuFe_2O_4$ (Ce4) showed the maximum gas sensitivity (86%) towards LPG with fast response time of 5 s and good recovery time of 68 s.

Keywords: D. Ferrite; Molten-salt method; TEM; Gas sensor

1. Introduction

The need of high performance solid state gas sensors has motivated several researchers in searching the new materials and investigating their gas sensing properties. Nowadays, semiconductor metal oxide sensors are extensively studied for their gas response property. Among these materials, the spinel type oxide semiconductors with formula AB_2O_4 like $NiFe_2O_4$, $CdFe_2O_4$ and $ZnFe_2O_4$ have been reported to be sensitive materials to both reducing and oxidizing gases [1–3]. $CuFe_2O_4$ is one of the most important ferrites and has a cubic close-packed arrangement of oxygen ions with $Cu^{2+}$and Fe^{3+} ions at two different crystallographic sites [4]. It has been extensively studied for its magnetic properties for the last few decades [5–7]. However, information on the gas-response properties of nanocrystalline $CuFe_2O_4$ to reducing gases is still limited. Therefore, it is interesting to investigate the gas-response properties of $CuFe_2O_4$. Chen et al. [8] reported $CuFe_2O_4$ sensor with excellent sensitivity towards acetylene. Tao et al. [9] observed that nanocrystalline $CuFe_2O_4$, by co-precipitation method, shows good response towards alcohol at operating temperature of 290 °C.

It is well known that, the gas-sensing efficiency of the material strongly depends on its microstructure, which in turn depends upon the method of preparation. The later part plays a vital role in view of the chemical and structural properties of the spinel ferrite. Also the response of the gas sensing material depends on various factors such as dopants, grain size, surface states, amount of adsorbed oxygen and its activation energy.

A variety of chemical methods have been reported for synthesis of ferrites which include ball-milling [5,6], combustion synthesis [7], co-precipitation [8,9], sol–gel [9], r.f. sputtering [10], solid state reaction [11] and molten-salt method [12,13]. Out of these methods, the molten-salt method is a convenient, environment friendly and inexpensive method for the preparation of ferrites at low processing temperature in short duration [13].

---

*Corresponding author. Tel.: +91 217 2744770.
E-mail address: sssuryavanshi@rediffmail.com (S.S. Suryavanshi).

0272-8842/$ - see front matter © 2013 Elsevier Ltd and Techna Group S.r.l. All rights reserved.
http://dx.doi.org/10.1016/j.ceramint.2013.01.010

The present research work deals with the preparation of nanocrystalline $CuFe_{2-x}Ce_xO_4$ ($x=0$, 0.04 and 0.08) and the effects of Ce doping on the structural, morphological and gas response properties have been investigated. To the best of our knowledge, this is the first attempt to synthesize Ce doped nanocrystalline $CuFe_2O_4$ materials by simple M-S method.

2. Experimental

Nanocrystalline undoped and Ce doped $CuFe_2O_4$ powders were prepared using the M-S synthesis route using sd-fine chemicals and analytical grade $Cu(SO_4)\cdot 5H_2O$, $Fe(NO_3)_3\cdot 9H_2O$, NaOH, NaCl and $Ce(NO_3)_2\cdot 6H_2O$ as precursor materials. The precursor materials were mixed in a molar ratio of 1:2:8:10 and ground together with an appropriate quantity of $Ce(NO_3)_2\cdot 6H_2O$ (0, 4 and 8 wt%) in agate mortar for nearly 30 min. The reaction between salts starts during the mixing process, accompanied by release of heat due to the exothermic reaction between the salts. As the reaction proceeded, the mixture became mushy and underwent a gradual change in color from greenish-red to brown. The resulting product was washed with deionized water several times to remove the unwanted salts formed during the reaction. The powder was dried under IR lamp for about 2 h and then calcined at 400 °C for 1 h to obtain nanocrystalline and homogeneously cation distributed particles. The reaction mechanism of formation of $CuFe_2O_4$ under the reaction conditions can be shown as follows [13–16]:

$$Cu(SO_4)\cdot 5H_2O + 2NaOH \overset{RT}{\rightarrow} CuO + Na_2SO_4 + 6H_2O \quad (1)$$

$$2Fe(NO_3)_3\cdot 9H_2O + 6NaOH \overset{RT}{\rightarrow} Fe_2O_3 + 6NaNO_3 + 12H_2O \quad (2)$$

$$CuO + Fe_2O_3 \rightarrow CuFe_2O_4 \quad (3)$$

In other words, $Cu(OH)_2$ and $Fe(OH)_3$ nanoparticles were first obtained from metallic salts and sodium hydroxides. Because of their smaller size and higher reaction activity, the freshly produced $Cu(OH)_2$ and $Fe(OH)_3$ decomposed immediately to produce CuO and Fe_2O_3 nanoparticles with a strong heat of reaction at room temperature (RT), thus $CuFe_2O_4$ was easily formed when the final powder was calcined even at temperature as low as 400 °C. The calcined $CuFe_2O_4$ powder was pelletized with manual hydraulic press machine using polyvinyl alcohol as a binder and at a pressure of $1.5\ \mathrm{t\,cm^{-2}}$. These disc shaped samples were sintered at 700 °C for 2 h at a heating rate of $2\ ^\circ\mathrm{C\,min^{-1}}$ in air to form ferrite through chemical reaction and then cooled down to RT at the same rate as that of heating. These sintered undoped (0%) and cerium doped (4% and 8%) samples are denoted as Ce0, Ce4 and Ce8, respectively. Conducting silver paste contacts (1 mm) were used to form ohmic contacts on the pellet sample. The gas sensing properties of the sintered pellets were measured using commercially developed gas sensing setup using bulk type sensor fabricated similar to that reported earlier [16,17]. The sensors were subjected to measurement of their electrical resistance in dry air or a test gas at various operating temperatures. The responses of the sensor were studied in a sealed test chamber (1 L capacity) with a gas inlet and an outlet. The test gas was injected into the test chamber through the inlet port and the resistance was measured as a function of time till a constant value was attained.

The temperature of the system was controlled from RT to 450 °C and two-probe dc measurement technique was used to measure the resistance of the sample in presence of air and with relevant test gases (LPG, acetone, ethanol and ammonia). The gas response is defined as

$$S(\%) = \frac{(R_a - R_g)}{R_a} \times 100 \quad (4)$$

where R_a is the resistance in air and R_g is the resistance in sample gas.

The structural studies of the sintered samples were characterized by using a Philips PW-3710 powder X-ray diffractometer with Cu K_α radiation with wavelength $\lambda = 0.154056$ nm. The crystallite size was calculated using Scherrer's formula ($D = 0.9\lambda/\beta\cos\theta$), where D is the average crystallite size, λ is the wavelength of X-ray used, β is the full width at half maximum (FWHM) of the most intense diffraction peak and θ is the peak position. The morphology of sintered samples was studied by scanning electron microscopy (SEM) with JEOL-JSM 6360, Japan model. The particle sizes of the sintered samples were observed using transmission electron microscopy (TEM) with PHILIPS CM-200 model.

3. Results and discussion

3.1. Structural studies

The structural changes and the identification of phases were investigated with the help of X-ray diffraction (XRD) technique. Fig. 1(a)–(c) shows the XRD patterns recorded over 20–90° for Ce0, Ce4 and Ce8 samples. XRD patterns reveal the formation of spinel-type $CuFe_2O_4$ with some additional peaks corresponding to Ce_2O_3 (JCPDS card no. 84-0310). Fig. 1(a) shows most of the observed peaks related to $CuFe_2O_4$. For Ce4 sample an intense (222) peak corresponding to the Ce_2O_3 phase appeared at 38° after cerium incorporation. However the (222) peak intensity is decreased for the Ce8 sample as compared to the Ce4 sample.

The average crystallite size was calculated according to Scherrer's formula and is shown in Table 1. We observed systematic reduction in the crystallite size of $CuFe_2O_4$ with Ce incorporation. The calculated crystallite sizes were found to be 38 nm, 26 nm and 11 nm for Ce0, Ce4 and Ce8 samples, respectively. It is observed that the crystallite size decreases with increasing Ce concentration, which is due to the formation of secondary phases, which hinders

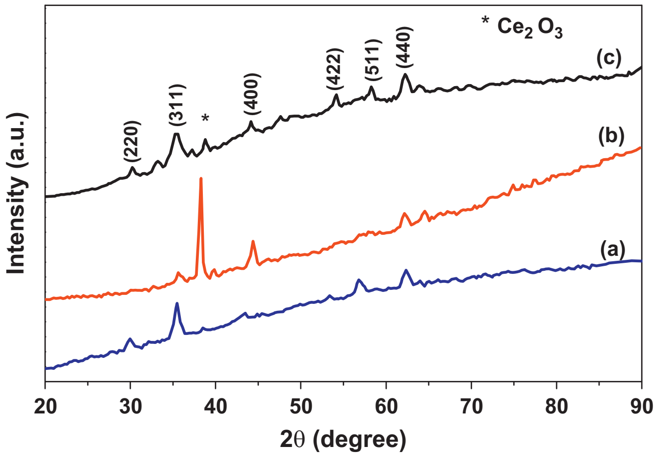

Fig. 1. X-ray diffraction patterns of (a) Ce0, (b) Ce4 and (c) Ce8 samples.

Table 1
The calculated crystallite size *D* (nm) and lattice parameter *a* (Å) of the Ce0, Ce4 and Ce8 samples.

Sample	Materials	Crystallite size (nm)	Lattice parameter (Å)
Ce0	$CuFe_2O_4$	38	8.400
Ce4	$CuCe_{0.04}Fe_{1.96}O_4$	26	8.413
Ce8	$Cu\ Ce_{0.08}Fe_{1.92}O_4$	11	8.426

the grain growth of the primary particles [18,19]. Also the observed lattice parameters after Ce doping are given in Table 1. This lattice parameters variation is due to their difference in the ionic radii.

3.2. Morphological studies

Fig. 2 shows SEM images for Ce0, Ce4 and Ce8 samples. SEM image for Ce0 sample (Fig. 2(a)) shows the formation of clusters i.e. aggregation of particles. It is seen that on addition of cerium the morphology varied systematically. Interestingly, for Ce4 sample the morphology changes markedly (Fig. 2(b)). It shows separated clusters of particles with voids and appears like cauliflowers grain growth. For Ce8 sample the grain size is still reduced, however it becomes more compact with overall less porosity (Fig. 2(c)). These results agree well with the Rezlescu et al. [20] observations, wherein they have shown 2 wt% Ce doped material exhibits well developed grains and their grain size was found to decrease with the increasing concentration of CeO_2 which hinders the grain growth. We observed that the lower grain size for Ce doped samples, which will be useful for gas sensing applications.

The typical TEM images for Ce0 and Ce8 samples are shown in Fig. 3 (a) and (b) respectively. The observed particle size for nanoparticles are varied between 30 and 60 nm (Fig. 3(a)). A significant reduction in particle size is also found from the TEM of Ce4 sample. It is clearly seen from the TEM image (Fig. 3(b)) that each particle size is less than 10 nm, which clearly remains isolated even after sintering at 700 °C. The structure also shows porosity with pores less than 5 nm size. The observed particle size from the TEM findings for these samples are well matched with the calculated average crystallite size from XRD. Such a low porosity and well distributed 8–10 nm sized particles are highly suitable for gas sensing application.

3.3. Gas-sensing properties

Fig. 4 shows the gas response for Ce0 sensor as a function of operating temperature. The Ce0 sensor showed a maximum response of 74% towards LPG at an operating temperature of 350 °C at 2000 ppm while it exhibited response of 58%, 34% and 22% towards acetone, ethanol and ammonia, respectively. The response time for Ce0 sensor is found to be 10 s and recovery time 2 min. The high response of $CuFe_2O_4$ towards LPG may be due to the formation of Cu^{1+} ions during the oxidation of reducing gas. In the inverse spinel $CuFe_2O_4$, Cu^{2+} ions prefer octahedral sites and Fe^{3+} ions are distributed on both octahedral (B) and tetrahedral (A) sites. The occurrence of the Cu^{2+} ion on the octahedral sites can provide greater number of hopping ($Fe^{2+} \leftrightarrow Fe^{3+}$, $Cu^{1+} \leftrightarrow Cu^{2+}$) on B sites and thus the gas response gets enhanced. Fig. 5 shows the variation in response with the test gas concentration for Ce0 sensor. It is found that the response increases with concentration from 100 ppm to 2000 ppm and it remains almost constant above 2000 ppm.

The gas response for Ce4 sensor is shown in Fig. 6. It shows maximum response of 86% towards LPG, while it shows 74% for acetone at 375 °C. It also exhibits gas response of 68% and 58% for ethanol and ammonia at 350 °C, respectively. The response time for the sensor is 5 s and recovery time 68 s. For Ce4 sensor, the increased gas response is attributed to the lower bulk density in comparison to Ce0 sensor. The variation in response with test gas concentration for Ce4 sensor is shown in Fig. 7. It is observed that the response increases with the concentration from 100 ppm to 2000 ppm and above 2000 ppm the response remains unaltered, indicating saturation level of test gases.

Fig. 8 depicts gas sensing characteristics for Ce8 sensor. It exhibits response of 69%, 61%, 55% and 51% towards LPG, acetone, ethanol and ammonia at operating temperatures of 325 °C, 375 °C, 375 °C and 425 ºC, respectively. It is found that the response decreases towards test gases for Ce8 sensor as compared to Ce4 sensor. As observed from the SEM image (Fig. 3(c)) shows the agglomeration of the nanoparticles observed for Ce8 sample. It prevents diffusion of oxygen into the bulk material which is responsible for the reduction in sensor response. This fact is also supported with the high density in comparison to the Ce4 sensor. The response time and the recovery time of the sensor are found to be 2 s and 58 s. Fig. 9 exhibits the variation of response with concentration

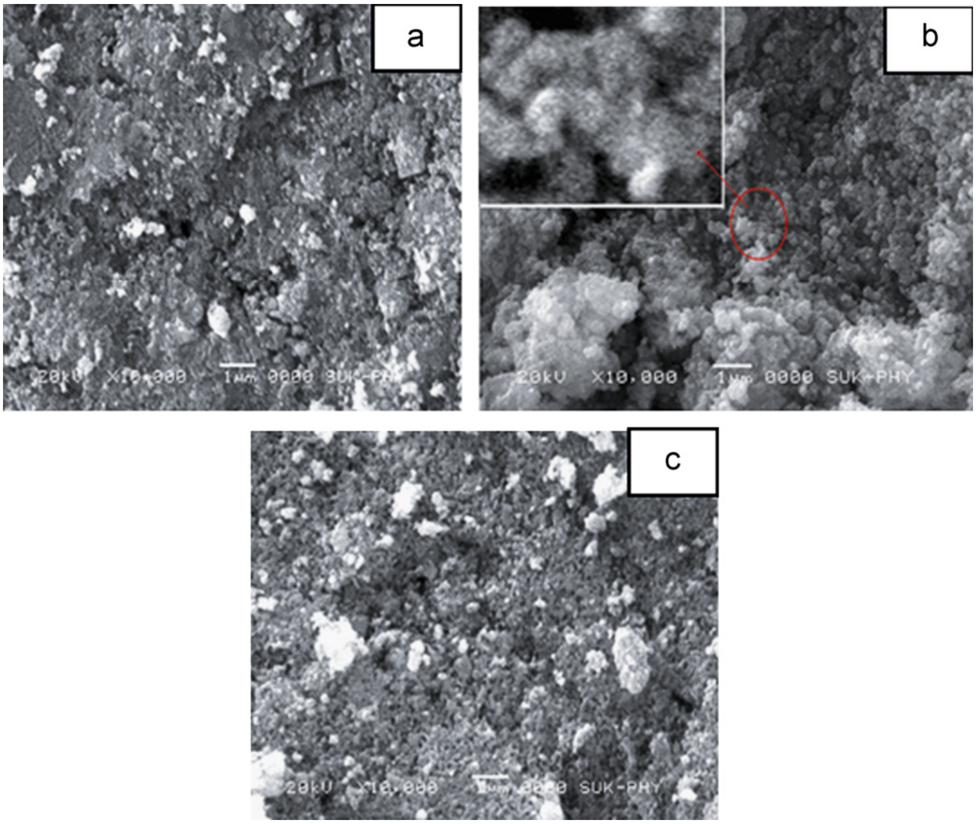

Fig. 2. SEM images of the (a) Ce0, (b) Ce4 and (c) Ce8 samples. Inset shows higher magnification image of the Ce4 sample.

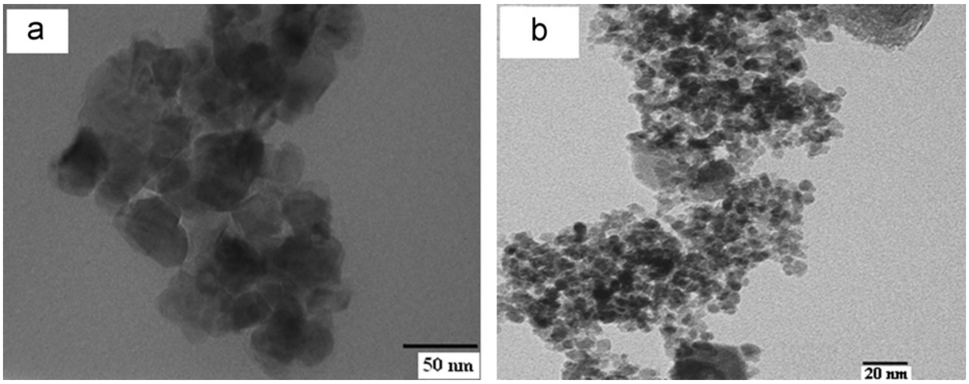

Fig. 3. TEM images of the (a) Ce0 and (b) Ce4 samples.

of test gas for Ce8 sensor. It is clear that the response is found to increase with concentration from 100 ppm to 2000 ppm and above 2000 ppm it remains almost constant, showing its saturation level. All the sensors discussed here exhibited short response and recovery time, within the range of 2–10 s and 1–2 min, respectively. In case of semiconducting metal oxide, sensing is a surface controlled process that is responsible for the sensitivity [21].

3.4. LPG sensing mechanism

The LPG sensing mechanism of the gas sensor is based on the change in the electrical resistance of the $CuFe_2O_4$ pellets resulting from the chemical reactions between LPG and adsorbed oxygen at the ferrite surface [22,23]. Both factors influence the kinetics of the chemisorption reaction between the sensor material and the surrounding gas. Better response would be expected if a larger amount of test gas is adsorbed and subsequently the reaction between the adsorbed reducing gas and the oxygen species is more favorable. The adsorption and ionization of oxygen from air or air containing the test gases can be expressed as [23–26]

$$O_{2\ \mathrm{gas}} \leftrightarrow O_{2\mathrm{ad}} \tag{5}$$

$$O_{2\mathrm{ad}} + e^- \rightarrow O_2^- \tag{6}$$

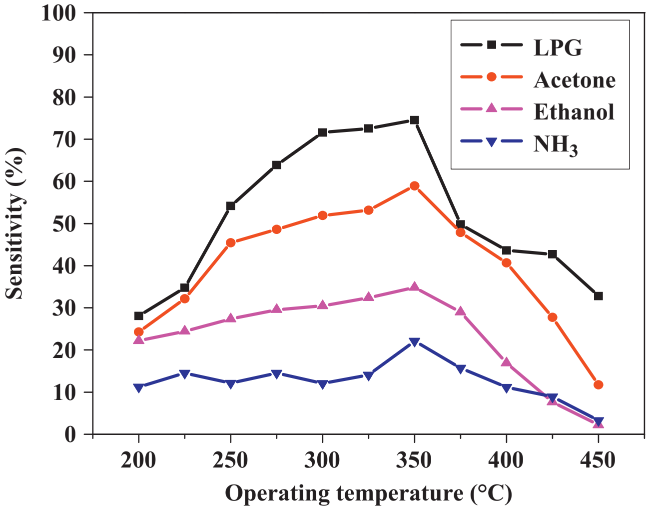

Fig. 4. Gas sensing response of Ce0 sensor towards the LPG, acetone, ethanol and ammonia gases.

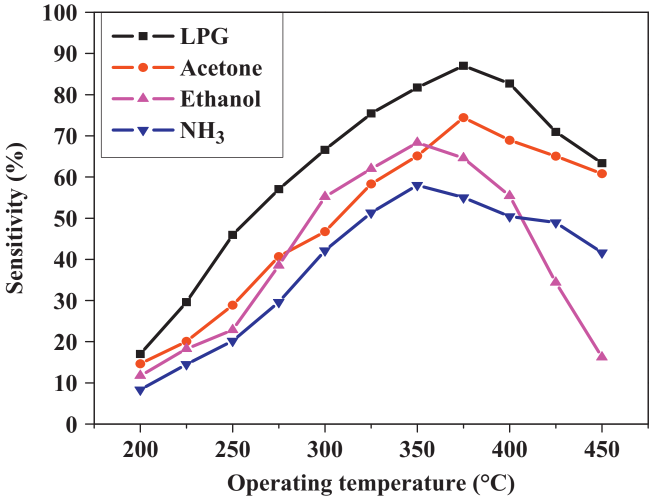

Fig. 6. Gas sensing response of Ce4 sensor towards the LPG, acetone, ethanol and ammonia gases.

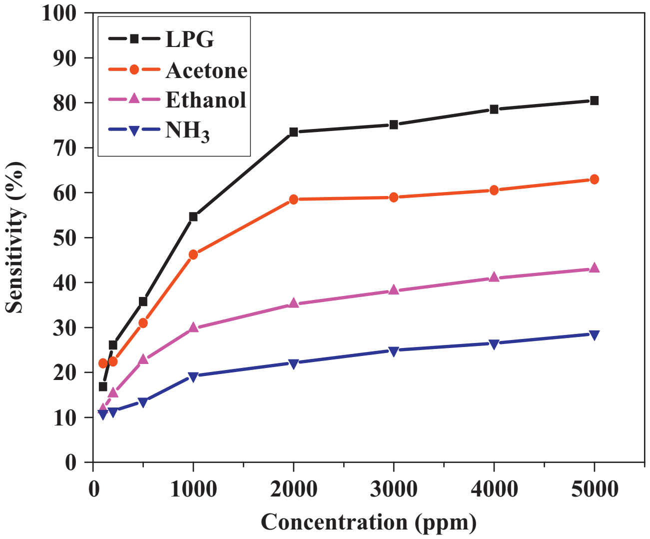

Fig. 5. Variation of gas sensitivity with concentration of test gas for Ce0 sensor.

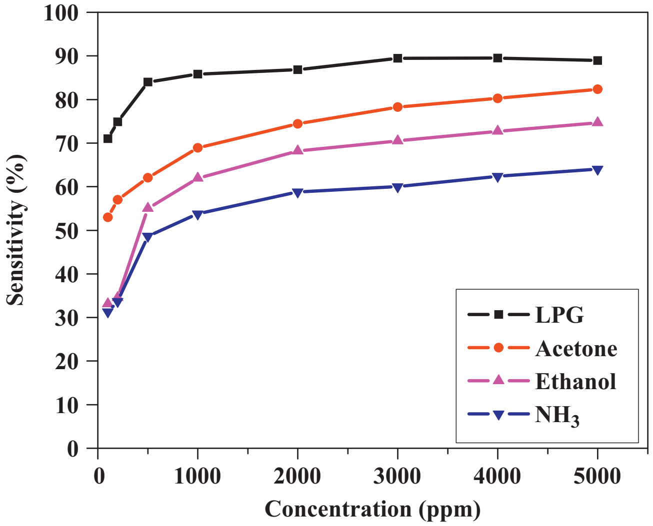

Fig. 7. Variation of gas sensitivity with concentration of test gas for Ce4 sensor.

It is observed that undoped and doped $CuFe_2O_4$ synthesized by M-S route exhibits better sensing response towards LPG. LPG is a mixture of hydrocarbon containing CH_4, C_3H_8 and C_4H_{10} wherein the reducing hydrogen species are bound to carbon atoms. Therefore, during the process of response at higher operating temperatures, LPG dissociates into reactive reducing components on the copper oxide surface. When such $CuFe_2O_4$ is exposed to LPG molecules, the hydrocarbons (C_nH_{2n+2}) of adsorbed LPG interacts with the pre-adsorbed oxygen. The reaction is given as

$$C_nH_{2n+2}+O_2^- \rightarrow C_nH_{2n}O+H_2O+e^- \quad (7)$$

From the reaction between LPG molecules and the pre-adsorbed O_2^-, the free electrons are released. These free electrons neutralize the holes from $CuFe_2O_4$, result in a decrease in the concentration of holes in $CuFe_2O_4$, and thus there is increase in resistance. The oxygen molecules from air are adsorbed on the $CuFe_2O_4$ surface while the interaction with LPG continuously forms water molecules to escape from the surface. When the flow of LPG was stopped for recovery, the oxygen molecules in air adsorbed on the surface of $CuFe_2O_4$, and the capture of electrons through the processes indicated in equations reduced the sensor resistance towards the initial stable surface state of $CuFe_2O_4$ [23].

With Ce incorporation, O_2 molecules dissociates at lower temperature and generates chemisorbed oxygen species much rapidly due to the enhanced interaction by Ce. Thus we achieved much higher response (86%)

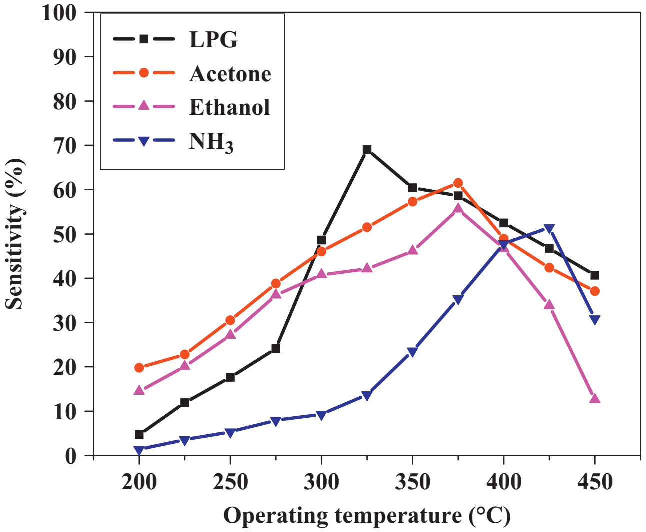

Fig. 8. Gas sensing response of Ce8 sensor towards the LPG, acetone, ethanol and ammonia gases.

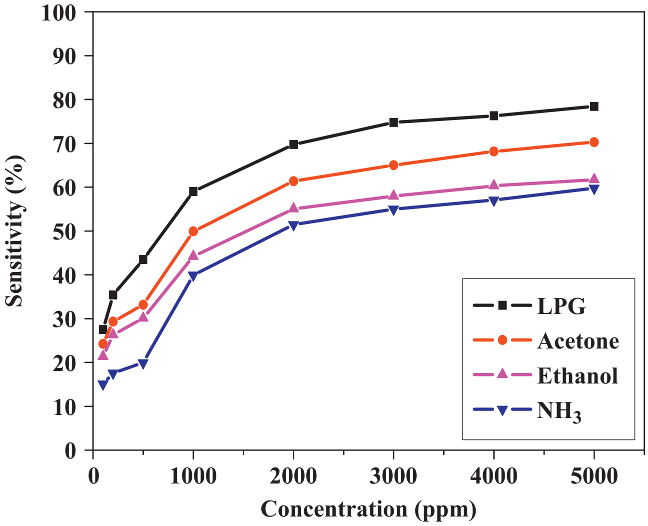

Fig. 9. Variation of gas sensitivity with concentration of test gas for Ce8 sensor.

observed from the cerium doped copper ferrite (Ce4 sample) at 375 °C.

3.5. *Response of the sensors towards 100 ppm concentration of test gases*

The gas response for Ce0, Ce4 and Ce8 sensors towards the 100 ppm concentration of LPG, acetone, ethanol and ammonia is shown in Fig. 10. It is seen that the Ce4 sensor exhibits remarkable response towards lower concentrations of LPG, acetone, ethanol and ammonia. Therefore the Ce4 sensor is found to be highly selective towards LPG at optimum temperature of 350 °C.

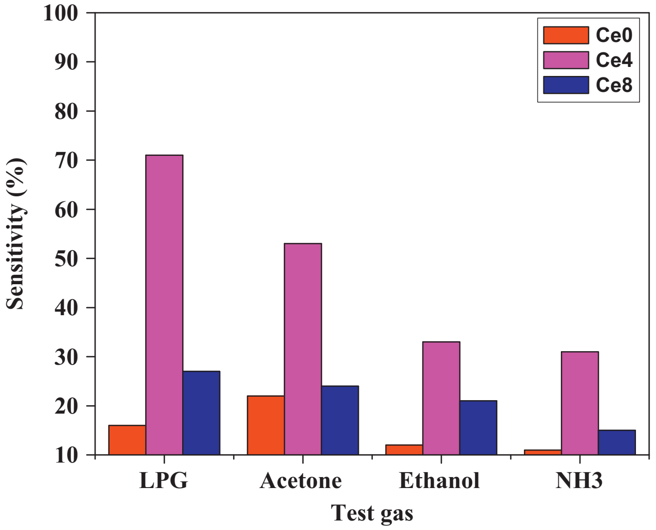

Fig. 10. Comparative gas responses (%) of Ce0, Ce4 and Ce8 sensors towards 100 ppm concentration of test gases at 350 °C.

4. Conclusions

Nanocrystalline undoped and Ce doped $CuFe_2O_4$ has been successfully synthesized by simple molten-salt method and effectively utilized as a reducing gas sensor element. Effects of Ce doping on the structural, surface morphological and gas sensing properties of copper ferrite were investigated. From XRD analysis the spinel $CuFe_2O_4$ ferrite structure was confirmed. The formation of nanoparticles was established from SEM and TEM investigations. The size of nanoparticles was decreased for the Ce doped samples. Sample Ce0 exhibited the selective response of 74% towards LPG at 2000 ppm at operating temperature of 350 °C. However after cerium incorporation, the sensitivity has been improved to 86% for Ce4 sample, while gas response decreased to 69% for Ce8 sample. Thus the present study explored the possibility of making use of cerium doped $CuFe_2O_4$ pellets for LPG sensing.

Acknowledgment

Authors gratefully acknowledge CSIR and DAE-BRNS, India for the financial support.

References

[1] L. Satyanarayana, K.M. Reddy, V.M. Sunkara, Nanosized spinel $NiFe_2O_4$: a novel material for the detection of liquefied petroleum gas in air, Materials Chemistry and Physics 82 (2003) 21–26.
[2] T.S. Zhang, P. Xing, J.C. Zhang, L.B. Kong, Ethanol-sensing characteristics of cadmium ferrite prepared by chemical coprecipitation, Materials Chemistry and Physics 61 (1999) 192–198.
[3] X. Chu, X. Liu, G. Meng, Preparation and gas sensitivity properties of $ZnFe_2O_4$ semiconductors, Sensors and Actuators B: Chemical 55 (1999) 19–22.
[4] S. Krupicka, P. Novak, E.P. Wohlfarth (Eds.), Handbook of Ferromagnetic Materials, vol. 3,1982, pp. 189–304.

[5] G.F. Goya, H.R. Rechenberg, Superparamagnetic transition and local disorder in $CuFe_2O_4$ nanoparticles, Nanostructured Materials 10 (1998) 1001–1011.

[6] J.Z. Jiang, G.F. Goya, H.R. Rechenberg, Magnetic properties of nanostructured $CuFe_2O_4$, Journal of Physics D: Condensed Matter 11 (1999) 4063–4078.

[7] P.B. Pandya, H.H. Joshi, R.G. Kulkarni, Magnetic and structural properties of $CuFe_2O_4$ prepared by the co-precipitation method, Journal of Materials Science Letters 10 (1991) 474–476.

[8] N.S. Chen, X.J. Yang, E.S. Liu, J.L. Huang, Reducing gas-sensing properties of ferrite compounds MFe_2O_4 (M = Cu, Zn, Cd and Mg), Sensors and Actuators B: Chemical 66 (2000) 178–180.

[9] S. Tao, F. Gao, X. Liu, O.T. Sørensen, Preparation and gas-sensing properties of $CuFe_2O_4$ at reduced temperature, Materials Science and Engineering B 77 (2000) 172–176.

[10] C. Despax, P. Tailhades, C. Baubet, C. Villette, A. Rousset, $CuFe_2O_4$ thin films: elaboration process, microstructural and magneto-optical properties, Thin Solid Films 293 (1997) 22–28.

[11] Z. Sun, L. Liu, D.Z. Jia, W. Pan, Simple synthesis of $CuFe_2O_4$ nanoparticles as gas-sensing materials, Sensors and Actuators B: Chemical 125 (2007) 144–148.

[12] S.L. Darshane, S.S. Suryavanshi, I.S. Mulla, Nanostructured nickel ferrite: a liquid petroleum gas sensor, Ceramics International 35 (2009) 1793–1797.

[13] S.L. Darshane, R.G. Deshmukh, S.S. Suryavanshi, I.S. Mulla, Gas-sensing properties of zinc ferrite nanoparticles synthesized by the molten-salt route, Journal of the American Ceramic Society 91 (2008) 2724–2726.

[14] X.R. Ye, D.Z. Jia, J.Q. Yu, X.Q. Xin, Z. Xue, One-step solid-state reactions at ambient temperatures—a novel approach to nanocrystal synthesis, Advanced Materials 11 (1999) 941–942.

[15] D.Z. Jia, J.Q. Yun, X. Xia, Synthesis of CuO nanometer powder by one step solid state reaction at room temperature, Chinese Science Bulletin 43 (1998) 571–573.

[16] Z.H. Jing, S.H. Wu, Preparation and gas sensing properties of γ-Fe_2O_3 nanopowders by solid-state grinding method at room temperature, Chinese Journal of Inorganic Chemistry 22 (2006) 483–487.

[17] R.C. Pawar, J.S. Shaikh, A.V. Moholkar, S.M. Pawar, J.H. Kim, J.Y. Patil, S.S. Suryavanshi, P.S. Patil, Surfactant assisted low temperature synthesis of nanocrystalline ZnO and its gas sensing properties, Sensors and Actuators B: Chemical 151 (2010) 212–218.

[18] R.K. Selvan, C.O. Augustin, V. Sepelak, L. John Berchmans, C. Sanjeeviraja, A. Gedanken, Synthesis and characterization of $CuFe_2O_4/CeO_2$ nanocomposites, Materials Chemistry and Physics 112 (2008) 373–380.

[19] A. Soldatov, T.S. Ivanchenko, S.D. Longa, A. Kotani, Y. Iwamoto, A. Bianconi, Crystal-structure effects in the Ce L_3-edge x-ray-absorption spectrum of CeO_2: multiple-scattering resonances and many-body final states, Physical Review B 50 (1994) 5074–5080.

[20] N. Rezlescu, E. Rezlescu, C. Pasnicu, M.L. Craus, Effects of the rare-earth ions on some properties of a nickel–zinc ferrite, Journal of Physics D: Condensed Matter 6 (1994) 5707–5716.

[21] X.Q. Liu, S.W. Tao, Y.S. Shen, Preparation and characterization of nanocrystalline α-Fe_2O_3 by a sol–gel process, Sensors and Actuators B: Chemical 40 (1997) 161–165.

[22] S. Singh, B.C. Yadav, R. Prakash, B. Bajaj, J.R. Lee, Synthesis of nanorods and mixed shaped copper ferrite and their applications as liquefied petroleum gas sensor, Applied Surface Science 257 (2011) 10763–10770.

[23] S. Singh, B.C. Yadav, V.D. Gupta, P.K. Dwivedi, Investigation on effects of surface morphologies on response of LPG sensor based on nanostructured copper ferrite system, Materials Research Bulletin 47 (2012) 3538–3547.

[24] K. Hara, N. Nishida, H_2 sensors using Fe_2O_3-based thin film, H_2 sensors using Fe_2O_4-based thin film, Sensors and Actuators B: Chemical 20 (1994) 181–186.

[25] X.H. Wu, Y.D. Wang, H.L. Liu, Y.F. Li, Z.L. Zhou, Preparation and gas sensing properties of perovskite-type $MSnO_3$ (M = Zn, Cd, Ni), Materials Letters 56 (2002) 732–736.

[26] S.C. Tsang, C.D.A. Bulpitt, P.C.H. Mitchell, A.J. Ramirez-Cuesta, Some new insights into the sensing mechanism of palladium promoted tin (IV) oxide sensor, The Journal of Physical Chemistry B 105 (2001) 5737–5742.